CHINESE JOURNAL OF CATALYSIS
Volume 33, Issue 2, 2012
Online English edition of the Chinese language journal

Cite this article as: Chin. J. Catal., 2012, 33: 237–246.

ARTICLE

Nanocasting, Template Synthesis, and Structural Studies on Cesium Salt of Phosphotungstic Acid for the Synthesis of Novel 1,3,5-Triaryl-pyrazoline Derivatives

Razieh FAZAELI[1,*], Hamid ALIYAN[2], Shahram TANGESTANINEJAD[1], Esmaeel MOHAMMADI[1], Maryam BORDBAR[3]

[1]Department of Chemistry, Shahreza Branch, Islamic Azad University, 86145-311, Iran
[2]Department of Chemistry, Mobarakeh Branch, Islamic Azad University, 84815-119, Iran
[3]Department of Chemistry, Faculty of Science, The University of Qom, 37185-359, Qom, Iran

Abstract: The elimination of the silica matrix of composites by HF occurred by a two-step reaction deposition of a $Cs_{2.5}H_{0.5}PW_{12}O_{40}$ (CsHPW) salt nanocrystal. We used 2D hexagonal SBA-15 silica as a template for the nanofabrication of CsHPW nanoparticles. Nanocast CsHPW materials are stable against leaching and colloidization in polar solvents. The catalytic performance of the nanocast CsHPW materials exceeded that of bulk $Cs_{2.5}H_{0.5}PW_{12}O_{40}$, which is the most active among the acidic HPW salts. A series of novel 1,3,5-triaryl-pyrazoline derivatives were synthesized by the reaction between chalcone and phenylhydrazine in high yield in the presence of CsHPW salt nanocrystals.

Key words: nanocasting; nanoparticle; green chemistry; 1,3,5-triaryl-2-pyrazoline; polyoxometalate

High-surface area inorganic materials have attracted widespread attention in diverse areas such as heterogeneous catalysis [1], adsorption [2–5], gas sensing [6,7], energy storage [8], drug delivery [9,10] biomedical applications [11], and electrochemistry [12–14] etc. Because of this broad range of applications much effort has been put into reviewing and updating the material's preparation methods [15–17]. The application of the nanocasting technique to the fabrication of inorganic compounds implies that the fabrication of these products takes place in the nanospaces provided by the pores of a porous solid (hard template). After the synthesis of the material, the template framework is selectively removed and an inorganic product is obtained.

Basically, the nanocasting route comprises three steps: (i) infiltration of the porous the template (i.e. SiO_2-SBA-15) with a solution containing the precursors of the inorganic compound; (ii) heat treatment under a controlled atmosphere of the impregnated template to convert the infiltrated precursor into an inorganic material and (iii) the removal of the template framework by dissolution (i.e. silica) or by oxidation under high temperatures (i.e. carbon) (Fig. 1). Because the synthesis takes place in a confined nanospace sintering of the particles is

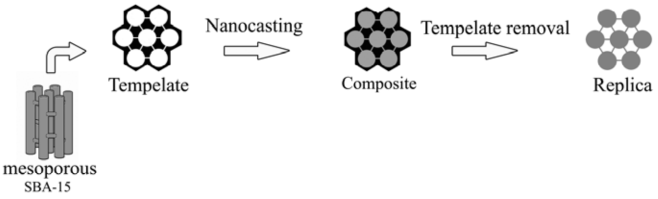

Fig. 1. Illustration of the nanocasting pathway.

Received 25 May 2011. Accepted 17 June 2011.

*Corresponding author. Tel: +98-321-3232706-7; Fax: +98-321-3232701-2; E-mail: fazaeli@iaush.ac.ir

This work was supported by Islamic Azad University, Shahreza Branch.

DOI: 10.1016/S1872-2067(11)60330-6

restricted and the preparation of high surface area materials (nanostructures or nanoparticles) is achieved. In this way, even though high (temperature) is required, numerous inorganic compounds with high surface areas can be obtained. Moreover, this synthetic strategy clearly suggests that the structure of the synthesized inorganic compounds can be tailored depending on the pore characteristics of the selected template [18].

Catalysis by polyoxometalates has attracted much attention because of their strong acidity and redox properties. An additional attractive aspect of polyoxometalates in catalysis is their inherent stability toward oxygen donors [19]. The practical application of the cesium salts of $CsPW_{12}O_{40}$ (denoted CsPW hereafter) have been limited by two factors: first is formation of milky suspensions in the polar substrates, which causes filtration problems for the liquid phase reactions and the second is a pressure drop in the fixed bed reactors [20]. Stabilizing them in a mesoporous matrix can help to overcome the drawbacks. Basically, they can support the catalytic phase and then be liberated from the matrix to form a nanocast. Reaction deposition is used to nanocoat the materials at different stages during the preparation of the CsHPW [21].

The real chemical composition of the CsHPW phase and its accessible surface within the supporting composite materials that determines the potential performance of the catalytic phase remains unknown. All the existing protons in bulk microporous CsHPW with a crystal size of 12 nm and a Cs/W_{12} ratio of 2.5 are available for the adsorption of NH_3 [22] and pyridine [23]. Therefore, a further increase in the acidity and catalytic activity can be expected by decreasing the crystal sizes to less than 10 nm. Also, diminishing the diffusion limitations of the reagents/products can increase the catalytic reaction rates because the diffusion limitations in microporous materials like zeolites are insignificant in this range of crystal sizes [24]. Recently, it was shown that the insertion of CsHPW into SBA-15 increases the absorbed ammonia more than 3 fold per gram of CsHPW phase [25].

Pyrazolines are well known and important nitrogen-containing five-membered heterocyclic compounds and various methods have been used for their synthesis [26]. Pyrazoline derivatives are attracting an increasing amount of interest in medicinal chemistry because of their bioactivity such as antimicrobial [27], antiamoebic [28], antinociceptive [29], anticancer [30], antidepressant [31], and anti-inflammatory [32] activity and also their use in conjugated fluorescent dyes as blue fluorescence emitters with a high fluorescence quantum yield [33] and a high electroluminescence yield [34]. Among the various pyrazoline derivatives, 1,3,5-triaryl-2-pyrazolines (TAP) seem to be the most frequently studied pyrazoline-type compounds. Several catalysts have been developed for the preparation of these heterocycles including sodium acetate-acetic acid aqueous solution under ultrasound irradiation [35], hot acetic acid solution [36], K_2CO_3-mediated microwave irradiation [37], $H_3PW_{12}O_{40}$ [38], and tungstophosphoric acid supported on highly organosoluble polyamide (PW_{12}/PA) [39].

As a part of our continuing effort to understand the catalytic properties of heteropoly acids (HPAs) [40–42], we report on the use of a nanoparticle catalyst for the synthesis of TAP derivatives (Scheme 1) and the introduction of a good application for $Cs_{2.5}H_{0.5}PW_{12}O_{40}$ (CsHPW).

1 Experimental

All materials were commercial reagent grade. Aldehydes, phenylhydrazine, acetophenone, and $H_3PW_{12}O_{40}$ (HPW) were purchased from Merck or Aldrich. Infrared spectra (FT-IR) (400–4000 cm^{-1}) were recorded using KBr pellets on a Nicolet Impact 400 D spectrometer. ^1H NMR spectra were obtained using a 300 MHz Bruker-Avance AQS. Melting points were determined using an electrothermal digital melting point apparatus and are uncorrected. Reaction courses and product mixtures were monitored by thin layer chromatography. X-ray powdered diffraction (XRD) patterns were obtained using a Bruker-D8 advance with automatic control. The patterns were run with monochromatic Cu K_α ($\lambda = 0.15406$ nm) radiation at a scan rate of 2°/min. Micrographs were recorded using a scanning electron microscope (SEM, HITACHI COM-S-4200) operated at an accelerating voltage of 30 kV. Thermogravimetric (TG) analyses were carried out on a Labsys-Setaram TGA-DSC instrument in flowing N_2 at a heating rate of 20 °C/min up to 1000 °C.

1.1 Materials

1.1.1 SBA-15

SBA-15 was first synthesized by Sun et al. [43] in 1998 using the amphiphilic triblock copolymers, $EO_{20}PO_{70}EO_{20}$ (Pluronic P123), as a template. In a typical synthesis, 1.00 g of P123 was dissolved in a mixture of HCl/H_2O (30.00 g of 2

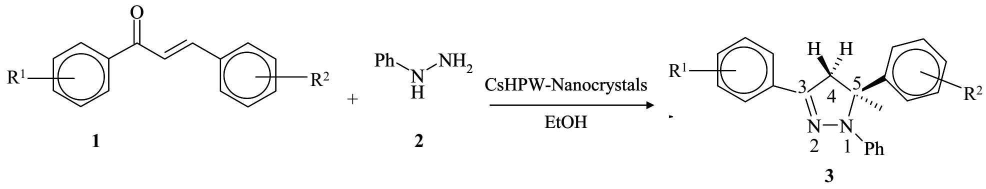

Scheme 1. Synthesis of 1,3,5-triaryl-2-pyrazolines.

mol/L HCl to 7.50 g H_2O). After dissolution 2.08 g of tetraethyl orthosilicate (TEOS) or 1.96 g of sodium silicate was added. The slurry was hydrothermally treated at 100 °C for 48 h after stirring at 40 °C for 16 h. The product was filtered and dried at 800 °C for 10 h.

1.1.2 CsHPW/SBA

CsHPW was inserted into the SBA-15 silica matrix by the two-step reaction deposition method. The parent CsHPW/SBA sample was obtained by dispersing surfactant-free SBA-15 (0.5 g) into 10 ml of *n*-propanol followed by the addition of 0.20 g of cesium carbonate. The contents were stirred for 4 h, filtered and dried under vacuum. The dry solids were treated for 12 h with a solution containing excess HPW dissolved in n-propanol under continuous stirring after which they were filtered and washed with excess *n*-propanol. The resulting solids were dried at 383 K for 2 h and calcined at 573 K for 2 h [21] (Fig. 2).

1.1.3 CsHPW nanoparticles

The silica matrix was gradually removed from the CsHPW/SBA materials by treatment with HF. The CsHPW/SBA composite 0.50 g was continuously stirred in 20 ml of an aqueous HF solution for 3 h at room temperature (Fig. 3). The solid was recovered by decantation after centrifugation (7000 r/min). The water addition/centrifugation sequence was repeated three times and finally the material was evacuated at 333 K [21].

1.2 General procedure for the synthesis of chalcone (benzylideneacetophenone)

To a 500 ml bolt-head flask with a mechanical stirrer 22.00 g of sodium hydroxide in 200 ml of water and 100.00 g (122.5 ml) of rectified spirit was added. To this mixture freshly distilled acetophenone (52.00 g, 0.43 mol) was added at 0 °C. After stirring for 5 min, 46.00 g (44 ml, 0.43 mol) of pure benzaldehyde was added. The temperature of the mixture was kept at about 25 °C (the requirement is 15–30 °C) and it was stirred vigorously until the mixture was thick enough for stirring to no longer be effective (2–3 h). The stirrer was removed and the reaction mixture was placed in an ice chest or refrigerator overnight. The product was filtered by suction using a Buchner funnel or a sintered glass funnel, washed with cold water until neutral to litmus followed by washing with 20 ml of ice-cold rectified spirit. The crude chalcone, after drying in air, weighed 88 g and melted at 50–54 °C. The chalcone was recrystallized from rectified spirit that was warmed to 50 °C (about 5 ml per gram) (Scheme 2) [44].

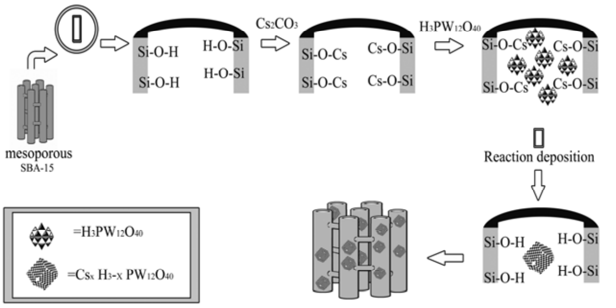

Fig. 2. Preparation of CsHPW/SBA.

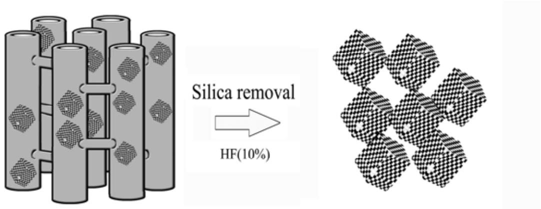

Fig. 3. Preparation of the CsHPW nanoparticles.

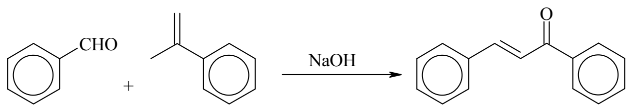

Scheme 2 Synthesis of chalcone.

1.3 Typical procedure for the synthesis of 1,3,5-triaryl pyrazoline

The following components were added to the reaction vessels: chalcone (1 mmol), phenylhydrazine (1 mmol), and CsHPW nanocrystals (0.03 mmol). Reaction progress was monitored by chin layer chromatography. At the end of the reaction the produced mixture was washed off the vessel using EtOAc (20 ml) and then it was filtered. The filtrate was dried ($MgSO_4$) and evaporated. The crude product was purified by column chromatography to provide 1,3,5-triaryl pyrazoline.

1.4 Selected spectroscopic data

5-(4-Methylphenyl)-1,3-diphenyl-2-pyrazoline (3c). ^{1}H NMR ($CDCl_3$): δ 2.34 (s, 3H, CH_3), 3.14 (dd, J = 7.1 Hz, 17.0 Hz, 1H), 3.85 (dd, J = 12.1, 17.0 Hz, 1H), 5.27 (dd, J = 6.9, 12 Hz, 1H) 6.77–7.75 (m, 14H). Anal. calcd. for $C_{22}H_{20}N_2$: C, 84.62; H, 6.41; N 8.97; found C, 84.61; H, 6.43; N, 9.00. ^{13}C NMR ($CDCl_3$): δ 21.68, 44.09, 64.73, 113.69, 119.47, 126.23, 128.43, 128.88, 129.34, 129.57, 130.19, 133.07, 137.67, 141.53, 145.43, 147.17. IR (KBr) $\nu_{\max}$ = 1117, 1499, 1593 cm^{-1}.

5-(4-Chlorophenyl)-1,3-diphenyl-2-pyrazoline (3d). ^{1}H-NMR ($CDCl_3$): δ 3.04 (dd, J = 7.4 Hz, 17.6 Hz, 1H), 3.77 (dd, J = 11.6 Hz, 17.6 Hz, 1H), 5.67 (dd, J = 7.4 Hz, 11.6 Hz, 1H), 6.71–7.64 (m, 14H); Anal. Calcd. for $C_{21}H_{17}ClN_2$: C, 75.78; H, 5.15; N, 8.41. Found: C, 75.69; H; 5.10; N, 8.49%. ^{13}CNMR ($CDCl_3$): δ 43.4, 63.8, 113.4, 119.4, 125.7, 127.3, 128.5, 128.7, 128.9, 129.3, 129.9, 132.5, 133.3, 141.1, 144.6, 146.7. IR (KBr) $\nu_{\max}$ = 1123, 1495, 1598 cm^{-1}.

5-(3-Chlorophenyl)-1,3-diphenyl-2-pyrazoline (3e). ^{1}H NMR ($CDCl_3$): δ3.08 (dd, J = 6.8 Hz, 17.0 Hz, 1H), 3.43 (dd, J = 12.2 Hz, 17.2 Hz, 1H), 5.63 (dd, J = 6.9 Hz, 12.4 Hz, 1H) 6.85–7.81 (m, 14H). Anal. calcd. for $C_{21}H_{17}N_2Cl$: C, 85.85; H, 5.72; N, 9.43; found C, 85.79; H, 5.70; N, 9.41. ^{13}C NMR ($CDCl_3$): δ 42.37, 61.54, 113.58, 119.60, 124.44, 127.79, 128.07, 128.92, 129.18, 129.48, 130.67, 132.53, 133.04, 135.04, 139.67, 144.84, 147.53. IR (KBr) $\nu_{\max}$ = 1127, 1501, 1593 cm^{-1}.

5-(2-Chlorophenyl)-1,3-diphenyl-2-pyrazoline (3f). ^{1}H NMR ($CDCl_3$): δ3.06 (dd, J = 4.8 Hz, 17.6 Hz, 1H), 3.96 (dd, J = 11.2 Hz, 17.7 Hz, 1H), 5.64 (dd, J = 4.7 Hz, 11.0 Hz, 1H), 6.76–7.74 (m, 14H); Anal. Calcd. for $C_{21}H_{17}ClN_2$: C, 75.78; H, 5.15; N, 8.41. Found: C, 75.83; H, 5.23; N, 8.38%.^{13}C NMR ($CDCl_3$): δ41.9, 61.5, 113.3, 119.2, 125.9, 127.5, 127.9, 128.3, 128.5, 128.8, 129.3. 129.8, 131.4, 132.2, 139.5, 144.6, 147.4. IR (KBr) $\nu_{\max}$ = 1120, 1497, 1595 cm^{-1}.

5-(2,4-Dichlorophenyl)-1,3-diphenyl-2-pyrazoline (3g). ^{1}H NMR ($CDCl_3$): δ 3.02 (dd, J = 6.6 Hz, 17.6 Hz, 1H), 3.97 (dd, J = 12.5 Hz, 17.5 Hz, 1H), 5.59 (dd, J = 6.6 Hz, 12.2 Hz, 1H), 6.69–7.71 (m, 13H); Anal. Calcd. for $C_{21}H_{16}Cl_2N_2$: C, 68.67; H, 4.39; N, 7.62. Found: C, 68.73; H, 4.39; N, 7.71%. ^{13}CNMR ($CDCl_3$): δ 41.5, 60.9, 113.5, 119.5, 124.3, 125.6, 127.4, 127.7, 128.6, 128.5, 128.5, 129.2, 129.5, 132.1, 133.9, 137.7, 144.4, 147.5. IR (KBr) $\nu_{\max}$ = 1118, 1503, 1589 cm^{-1}.

5-(3-Bromophenyl)-1,3-diphenyl-2-pyrazoline (3h). ^{1}H NMR ($CDCl_3$): δ3.08 (dd, J = 7.1 Hz, 17.0 Hz, 1H), 3.35 (dd, J = 12.1 Hz, 16.9 Hz, 1H), 5.68 (dd, J = 6.9 Hz, 12.7 Hz, 1H) 6.80–7.75 (m, 14H). Anal. calcd. for $C_{21}H_{17}N_2Br$: C, 85.85; H, 5.72; N, 9.43; found C, 85.78; H, 5.69; N 9.43. ^{13}C NMR ($CDCl_3$): δ 42.35, 60.47, 113.35, 119.50, 124.23, 127.94, 128.05, 129.06, 129.16, 129.35, 130.59, 132.41, 133.18, 139.66, 145.25, 147.14. IR (KBr) $\nu_{\max}$ = 1126, 1502, 1598 cm^{-1}.

5-(4-Methoxyphenyl)-1,3-diphenyl-2-pyrazoline (3i). ^{1}H NMR ($CDCl_3$): δ 3.12 (dd, J = 7.1 Hz, 17.1 Hz, 1H), 3.82 (s, 3H, OCH_3), 3.87 (dd, J = 12.1 Hz, 16.9 Hz, 1H), 5.24 (dd, J = 7.2 Hz, 12 Hz, 1H) 6.75–7.85 (m, 14H). Anal. calcd. for $C_{22}H_{20}N_2O$: C, 84.62; H, 6.41; N, 8.97; found C, 84.56; H, 6.40; N, 8.93. ^{13}C NMR ($CDCl_3$): δ 44.08, 55.64, 64.14, 113.72, 114.46, 119.54, 126.42, 127.91, 128.47, 128.89, 129.19, 130.56, 133.21, 135.03, 145.34, 147.17. FT-IR (KBr) $\nu_{\max}$ = 1120, 1261, 1512, 1597 cm^{-1}.

3-(4-Chlorophenyl)-1,5-diphenyl-2-pyrazoline (3j). ^{1}H NMR (DMSO): δ3.15 (dd, J = 7.1 Hz, 17.0 Hz, 1H), 3.87 (dd, J = 12.2 Hz, 17.1 Hz, 1H), 5.33 (dd, J = 7.3 Hz, 12.4 Hz, 1H) 6.83–7.67 (m, 14H). Anal. calcd. for $C_{21}H_{17}N_2Cl$: C, 84.85; H, 5.72; N, 9.43; found C, 84.81; H, 5.77; N, 9.47. ^{13}C NMR (DMSO): δ 42.39, 61.31, 113.53, 117.26, 126.83, 126.94, 128.64, 129.16, 129.39, 130.55, 132.17, 132.19, 136.05, 139.61, 143.73, 147.39. IR (KBr) $\nu_{\max}$ = 1121, 1509, 1599 cm^{-1}.

2 Results and discussion

2.1 Characterization of the CsHPW

FT-IR spectroscopy is a convenient method for the characterization of the Keggin structure of heteropolyanions. The infrared spectrum of the $Cs_{2.5}H_{0.5}PW_{12}O_{40}$ nanocasts (Fig. 4(c)) gave strong vibrations at 1081 (ν_{as}(P–Oa)), 986 (ν_{as}(W–Oa)), 892 (ν_{as}(W–O–W)), and 800 cm^{-1} (ν_{as}(W–Oc–W)) while bulk-$Cs_{2.5}H_{0.5}PW_{12}O_{40}$ gave vibrations at 1080, 986, 891, and 801 cm^{-1} (Fig. 4(a)). In addition, the observed band at 523 cm^{-1} may be attributed to the δ(P–O) vibration [45]. Moreover, the band located at 1622 cm^{-1} may be characteristic of the O–H stretching vibration (Fig. 4(c)).

The chemical composition of the bulk CsHPW samples and their nanocasts were estimated by averaging the results of energy dispersive X-ray spectroscopy (EDS) experiments at five different positions in the samples. EDS results indicate that the as-prepared CsHPW nanocast samples contain Cs, W, P, and O (Fig. 5 and Table 1). The percentage of silica matrix removed from the CsHPW/SBA composite was about 99%. The Cs content in the CsHPW materials was characterized by Cs/W_{12} further defined as the Cs/W_{12} ratio and this was calculated from the atomic percentages of Cs and W in the samples

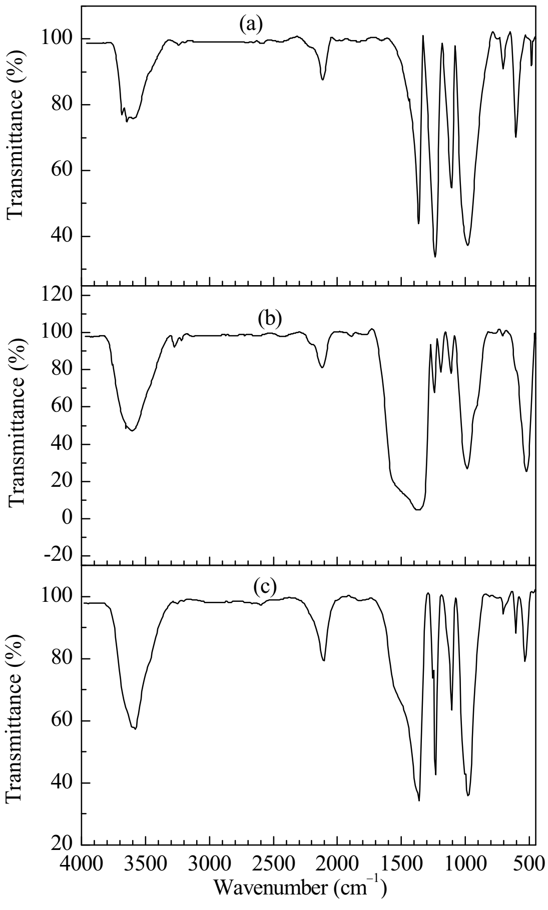

Fig. 4. FT-IR spectra of Bulk-CsHPW (a), CsHPW/SBA-15 (b), and CsHPW nanocrystals (c).

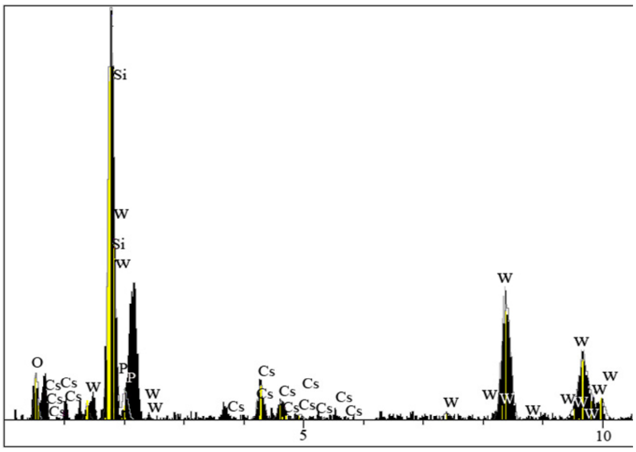

Fig. 5. EDS profile of CsHPW nanocast sample.

Table 1 EDS measurements carried out during the SEM observations

Element	Line	Intensity (c/s)	Conc (wt%)
O	Ka	32.54	1.788
Si	Ka	26.28	0.954
P	Ka	24.71	1.177
Cs	La	38.85	12.525
W	La	170.03	83.556

according to the EDS data. The good distribution of all the analyzed elements is in agreement with the atomic adsorption analysis, the neutron activation analysis (NAA) and ICP results with deviations of ±0.09. During the removal of silica the excess cesium located within the micropores transfers to the solution as it is dissolved in aqueous HF together with the silica matrix. Cesium was indeed found in the filtrate of this solution by atomic adsorption analysis. A SEM micrograph of CsHPW is shown in Fig. 6. No defined morphology is apparent for the particles but their edges appear to be spherical with diameters of about 43 nm. Isolated primary 10–20 nm nanoparticles of CsHPW were also present in the TEM micrographs (Fig. 7). However, isolated 5–9 nm nanoparticles of CsHPW were clearly observed by HRTEM in the curved nanotubular channels within the silica microfibers [21].

The thermal stability of $Cs_{2.5}H_{0.5}PW_{12}O_{40}$ was investigated for the crystalline samples under a N_2 atmosphere from 50 to 700 °C (Fig. 8). The TGA curve indicates that the weight loss of CsHPW can be divided into two steps. The first weight loss of 1.701% from 48 to 84 °C involves the release of three lattice water molecules. The second step beginning at about 465–518 °C (6.333%) is because of the decomposition of POM and the release of WO_3.

XRD analysis is widely used to study the structure of heteropoly complexes. XRD patterns of the as-prepared CsHPW/SBA-15 composite and the CsHPW nanocasts are shown in Fig. 9. The XRD peaks for the CsHPW phase within the CsHPW/SBA-15 composites (Fig. 9(1)), the bulk-CsHPW [21] and the CsHPW nanocasts (Fig. 9(2)) can be attributed to their bcc cubic structure, which is commonly associated with pure alkaline heteropoly salts [44]. Therefore, the removal of the silica matrix does not affect the crystal structure. The wide amorphous halo centered at $2\theta = 23°$ in the spectrum of SBA-15 silica in the as-prepared composites completely disappeared for the nanocasted materials.

The UV-Vis spectrum of the CsHPW nanocast is shown in Fig. 10. The two bands near 208 and 266 nm are attributed to $O_t \rightarrow W$ and μ_2-$O \rightarrow W$ ligand-to-metal charge transfer, respectively. Electrons are promoted from the low energy electronic states that are mainly composed of oxygen 2*p* orbitals to high-energy states that are mainly composed of metal *d* orbitals.

N_2 adsorption-desorption isotherms and the corresponding BJH pore size distribution curves for bulk-CsHPW,

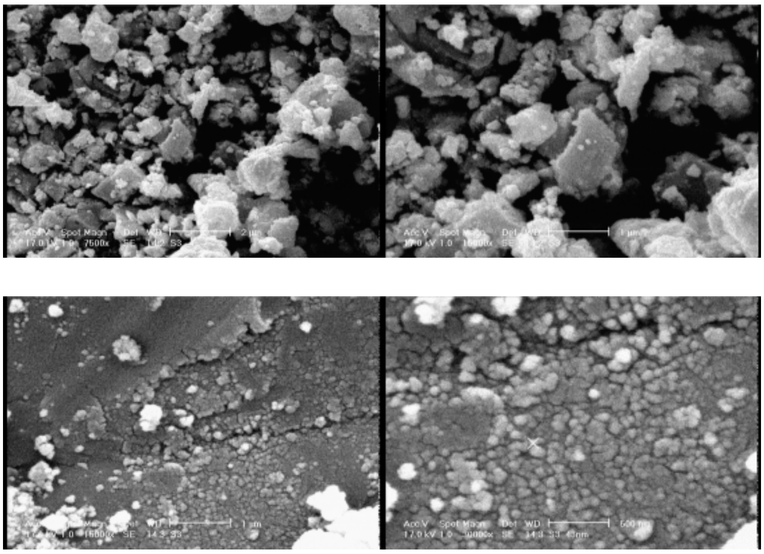

Fig. 6. SEM micrographs of the CsHPW nanoparticles.

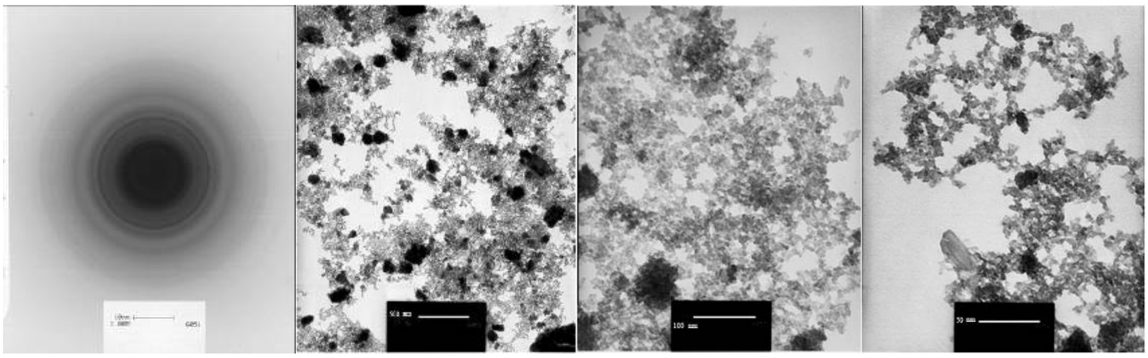

Fig. 7. TEM micrographs of the CsHPW nanocast.

CsHPW/SBA-15 and nanocast CsHPW materials are shown in Fig. 11. The isotherms for the CsHPW/SBA-15 exhibit type IV isotherm according to the IUPAC nomenclature [46] and this is a typical characteristic of mesoporous materials [47,48]. The physical properties of SBA-15, bulk-CsPW, CsPW/SBA-15, and CsPW nanocast are listed in Table 2. As expected, the BET surface areas, total pore volumes, and mesopore sizes of the SBA-15 [21] material decrease from 873 to 439 m^2/g, 1.4 to 0.74 cm^3/g and 6.4 to 5.8 nm, respectively, after functionalization with CsHPW. These changes reflect the part of the mesopore volume in the SBA-15 matrix that is filled with CsHPW nanocrystals resulting in pore diameters that are less than that of silica channels. After the removal of the silica matrix the nitrogen sorption isotherms of the CsHPW nanocast changed to a type I shape with small slopes for the plateau and a H4 hysteresis loop, as shown in Fig. 11.

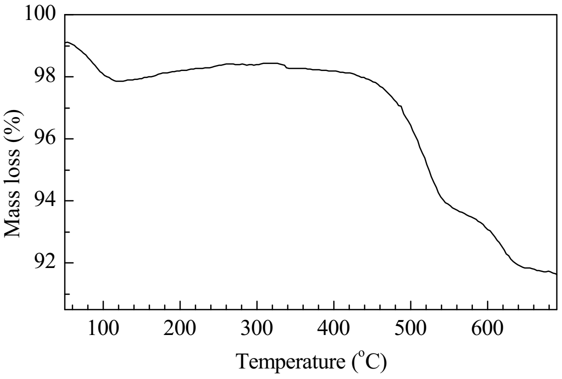

Fig. 8. TG analysis of the $Cs_{2.5}H_{0.5}PW_{12}O_{40}$ nanoparticles.

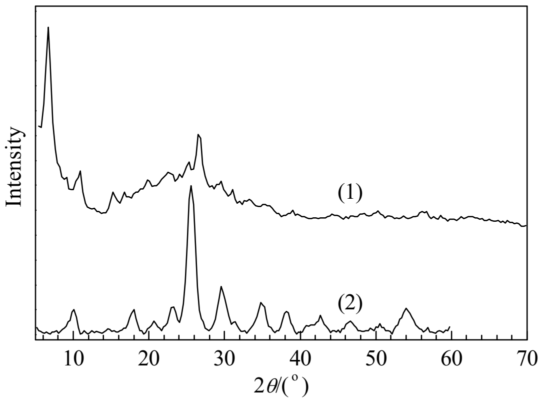

Fig. 9. XRD patterns of CsHPW/SBA-15 (a) and the $Cs_{2.5}H_{0.5}PW_{12}O_{40}$ (b) nanoparticles.

2.2 Choice of reaction media and effect of the catalyst on the synthesis of TAP derivatives

Initially, the condensation reaction between chalcone and phenylhydrazine was performed in the presence of a catalytic amount of two polyoxometalate (POM) Cs salts (Table 3, entries 1,2). The synthesis was not successful in the absence of the catalyst. The performance of the CsHPW/SBA-15 composite is shown in Table 3. Critically, the removal of silica caused an increase in reactivity (Table 3, entries 4–6). To determine the most appropriate medium for this heterocyclization reaction, the synthesis of TAP from the condensation between

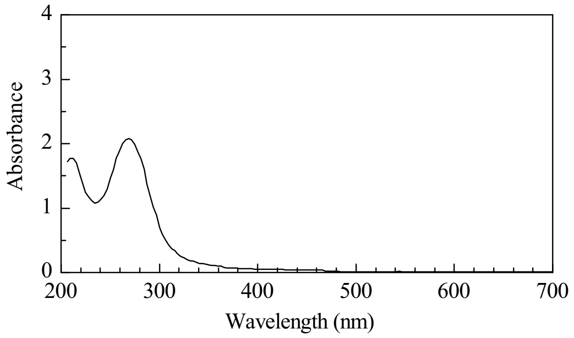

Fig. 10. UV-Vis spectrum of the CsHPW nanocasts.

Table 2 Texture parameters of the parent CsHPW/SBA-15 and CsHPW nanocasts and a comparison with bulk CsHPW materials

Material	Surface area[a] (m^2/g)	Pore volume[a] (cm^3/g)	Pore diameter (nm)
SBA-15 [21]	873	1.4	6.4
Bulk-CsHPW	19.336	0.3211	3.7672
CsHPW/SBA-15	439.29	0.7415	5.8337
CsHPW nanocast	83.825	0.2180	3.89

[a] Total pore volume measured at $p/p_0 = 0.99$.

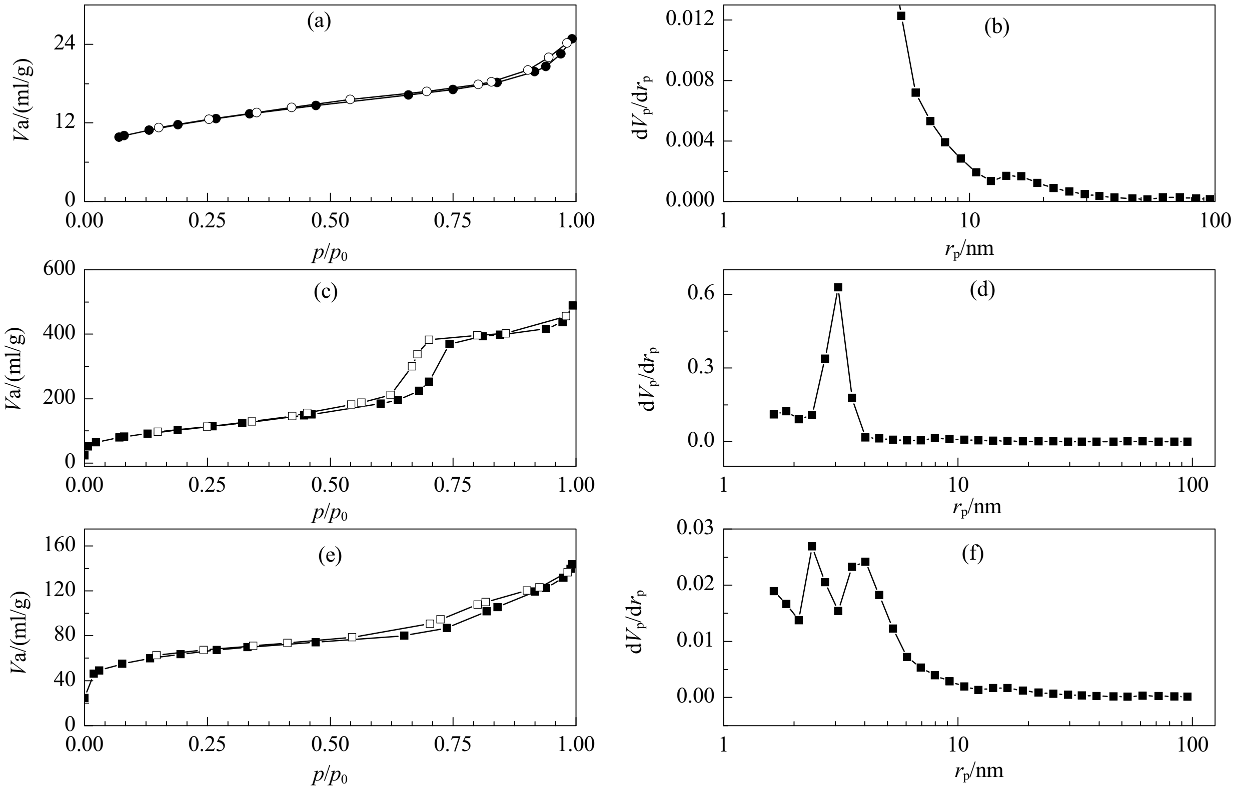

Fig. 11. N_2 adsorption-desorption isotherms and BJH pore sizes obtained from the adsorption branches recorded with bulk-CsPW (a, b), CsPW/SBA-15 (c, d), and CsPW nanocast (e, f).

chalcone and phenylhydrazine in the presence of a catalytic amount of CsHPW nanoparticles was selected as a model reaction. Alcoholic solvents (methanol and ethanol), CH_2Cl_2, CH_3CN, and $CHCl_3$ gave good conversions (Fig. 11). Clearly, ethanol stands out as the solvent of choice with its fast conversion, high yield, and easy removal. To establish the optimal conditions, a set of experiments was carried out by varying the amount of catalyst (Table 3, entries 3–5). The feed ratios of the reaction (Table 3, entries 4,7,8) and (Fig. 11 and Table 3) were varied as well. The best conditions for the preparation of TAP derivatives were achieved when 1 mol chalcone, 1 mol phenylhydrazine, and 0.03 mol CsHPW nanoparticles were used. These conditions were applied to a series of substituted aromatic aldehydes.

On the basis of the above results, to extend the scope and generality of this method several structurally diverse chalcones and phenylhydrazines were cyclized to give TAP using CsHPW nanocrystals. The results are listed in Table 4 and the reactions proceeded well with all the substrates but the substrates with electron-donating groups were generally more reactive than those with electron-withdrawing groups.

To show the effect of CsHPW nanocrystal catalytic activity on the synthesis of TAP derivatives, all the reactions were repeated using the same reaction conditions in the presence of $H_3PW_{12}O_{40}$ [38] and PW_{12}/PA [39] as catalysts. The obtained results showed that the turnover frequencies (TOF) for the synthesis of the 1,3,5-triarylpyrazoline derivatives that were catalyzed by the CsHPW nanocrystals were higher than that of PW_{12} and PW_{12}/PA. One explanation for this behavior is that the CsHPW nanocrystals have high specific structure areas.

We then attempted to prepare other types of 2-pyrazolines using the above-mentioned optimum conditions. When aldehyde **4**, methyl acetoacetate **5**, phenylhydrazine **2,** and

Table 3 Effect of different conditions on the reaction between chalcone and phenylhydrazine at 45 °C

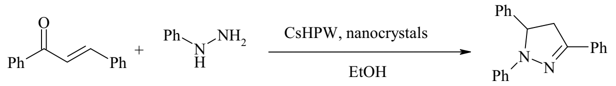

Entry	Catalyst	Catalyst amount (mol%)	Isolated yield (%)
1	Bulk-CsHPW	3	68
2	Bulk-CsHPMo	3	45
3	CsHPW/SBA-15	4	86
4	CsHPW-nanocrystals	3	92
5	CsHPW-nanocrystals	2	78
6	CsHPW-nanocrystals	4	92
7	CsHPW-nanocrystals[a]	3	82
8	CsHPW-nanocrystals[b]	3	80

Reaction conditions: chalcone (1 mmol), phenylhydrazine (1 mmol), and catalyst (0.03 mmol) in EtOH (5 ml) over 2 h at 45 °C.

[a] Chalcone/phenylhydrazine: 1/2.

[b] Chalcone/phenylhydrazine: 1/3.

Table 4 Synthesis of TAP derivatives in the presence of CsHPW nanocrystals

TAP	R$_1$	R$_2$	Isolated yield (%)[b]	TON	TOF	Melting point (°C)	
						Found	Reported
3a	H	H	95	3.135	9.5	130–132	134–135 [37]
3b	H	4-NO$_2$	90	2.970	9.0	136–138	—
3c	H	4-Me	98	3.234	9.8	128–130	128–130 [35]
3d	H	4-Cl	90	2.970	9.0	136–137	133–134 [36]
3e	H	3-Cl	85	2.805	8.5	131–133	134–136 [35]
3f	H	2-Cl	87	2.871	8.7	131–133	134–135 [36]
3g	H	2,4-Cl$_2$	90	2.97	9.0	136–138	—
3h	H	3-Br	92	3.036	9.2	139–141	141–143 [35]
3i	H	4-MeO	>98	3.234	9.8	109–111	110–112 [35]
3j	4-Cl	H	92	3.036	9.2	143–145	143–145 [35]
3k	4-Br	H	85	2.805	8.5	144–147	—

Reaction conditions: chalcone (1 mmol), phenylhydrazine (1 mmol) and CsHPW (0.03 mol) in EtOH over 20 min.

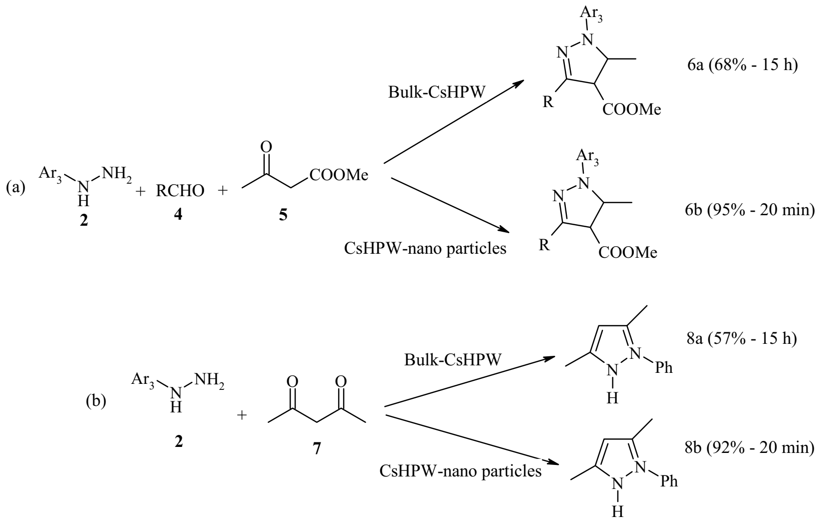

Scheme 3. Preparation of 2-pyrazolines using CsHPW.

bulk-CsHPW (Scheme 3) or acethyl acetonate **7** (1,3-diketone), phenylhydrazine, and bulk-CsHPW were used the corresponding 2-pyrazolines (**6a**, **8a**) were obtained in 68% and 57% yields, respectively (Scheme 2). However, in the presence of catalytic amounts of CsHPW nanocrystals the corresponding 2-pyrazolines (**6b**, **8b**) were obtained in EtOH as solvent in 95% and 92% yields after 20 min, respectively.

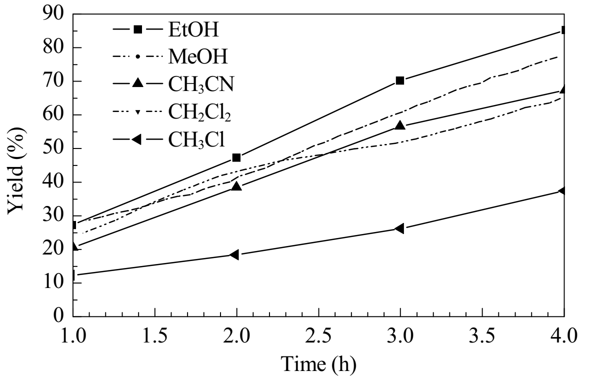

Fig. 12. Effect of various solvents in the reaction between chalcone with phenylhydrazine at room temperature. Reaction conditions: chalcone (1 mmol), phenylhydrazine (1 mmol) and catalyst (0.03 mmol) in solvent (5 ml) over 4 h.

3 Conclusions

The preparation of CsHPW salts, supported on mesostructured SBA-15 silica, by the reaction deposition strategy causes the formation of isolated CsHPW nanocrystals within the nanotubular channels. A remarkable characteristic of the SBA-15 structure is that all the cylindrical pores are connected by small channels. This results in a completely three-dimensional SBA-15 pore system. We have developed an efficient strategy for the synthesis of 1,3,5-triaryl pyrazoline and 2-pyrazolines using CsHPW nanoparticles as an eco-friendly, inexpensive and efficient catalyst. The advantages of this catalytic system are mild reaction conditions, short reaction times, high product yields, easy catalyst preparation, non-toxicity of the catalysts, and a simple and clean work-up of the desired products.

References

1 Raimondi F, Scherer G G, Ko¨tz R, Wokaun A. *Angew Chem*, *Int Ed*, 2005, **44**: 2190

2 Medine G M, Zaikovskii V, Klabunde K J. *J Mater Chem*, 2004, **14**: 757

3 Carnes C L, Stipp J, Klabunde K J, Bonevich J. *Langmuir*, 2002, **18**: 1352

4 Carnes C L, Kapoor P N, Klabunde K J, Bonevich J. *Chem Mater*, 2002, **14**: 2922

5 Rajagopalan S, Koper O, Decker S, Klabunde K J. *Chem Eur J*, 2002, **8**: 2602

6 Reddy K M, Satyanarayana L, Manorama S V, Misra R D K. *Mater Res Bull*, 2004, **39**: 1491

7 Rossinyol E, Arbiol J, Peiro F, Cornet A, Morante J R, Tian B, Bo T, Zhao D. *Sens Actuators B*, 2005, **109**: 57

8 Arico A S, Bruce P, Scrosati B, Tarascon J M, Van Schalkwijk W. *Nat Mater*, 2005, **4**: 366

9 Barbe C, Bartlett J, Kong L G, Finnie K, Lin H Q, Larkin M, Calleja S, Bush A, Calleja G. *Adv Mater*, 2004, **16**: 1959

10 Yi D K, Selvan S T, Lee S S, Papaefthymiou G C, Kundaliya D, Ying J Y. *J Am Chem Soc*, 2005, **127**: 4990

11 Tartaj P, Morales M D P, Veintemillas-Verdaguer S, Gonzalez-Carreno T, Serna C J. *J Phys D Appl Phys*, 2003, **36**: R182

12 lvarez S A, Blanco-Lopez M C, Miranda-Ordieres A J, Fuertes A B, Centeno T A. *Carbon*, 2005, **43**: 866

13 Fuertes A B, Lota G, Centeno T A, Frackowiak E. *Electrochim Acta*, 2005, **50**: 2799

14 Lee J, Yoon S, Hyeon T, Oh S M, Kim K B. *Chem Commun*, 1999: 2177

15 Schuth F. In: Schuth F, Singh K S W, Weitkamp J ed. Handbook of Porous Solids, Vol. 1. Weinheim: Wiley-VCH, 2002. 535

16 Landau M V. In: Schu th F, Singh K S W, Weitkamp J ed. Handbook of Porous Solids. Weinheim: Wiley-VCH, 2002. 1677

17 Weidenkaff A. *Adv Eng Mater*, 2004, **6**: 709

18 Valdes-Solıs T, Fuertes A B. *Mater Res Bull*, 2006, **41**: 2187

19 Neumann R. *Prog Inorg Chem*, 1998, **47**: 317

20 Okuhara T, Kimura M, Kawai T, Xu Z, Nakato T. *Catal Today*, 1998, **45**: 73

21 Madhusudhan Rao P, Goldberg-Oppenheimer P, Kababya S, Vega S, Landau M V. *J Mol Catal A*, 2007, **275**: 214

22 Okuhara T, Watanabe H, Nishimura T, Inumaru K, Misono M. *Chem Mater*, 2000, **12**: 2230

23 Dias J A, Caliman E, Dias S C L. *Microporous Mesoporous Mater*, 2004, **76**: 221

24 Landau M V, Vradman L, Valtchev V, Lezervant J, Liubich E, Talianker M. *Ind Eng Chem Res*, 2003, **42**: 2773

25 Rao P M, Landau M V, Wolfson A, Shapira-Tchelet A M, Herskowitz M. *Microporous Mesoporous Mater*, 2005, **80**: 43

26 Wiley R H, Ed.; Pyrazoles, Pyrazolines, Pyrazolidines, Indazoles and Condensed Rings; in the Chemistry of Heterocyclic Compounds; Weissberger A, Ed.; Interscience Publishers: New York, 1967; Vol. 22, p 180

27 Manna K, Agrawal Y K. *Bioorg Med Chem Lett*, 2009, **19**: 2688

28 Abid V, Bhat A R, Athar V, Azam A. *Eur J Med Chem*, 2009, **44**: 417

29 Kaplancikli Z A, Turan-Zitouni G, Özdemir A, Devrim Can Ö, Chevallet P. *Eur J Med Chem*, 2009, **44**: 2606

30 Havrylyuk D, Zimenkovsky B, Vasylenko O, Zaprutko L, Gzella A, Lesyk R. *Eur J Med Chem*, 2009, **44**: 1396

31 Gokhan-Kelekc N, Koyuno glu S, Yabano glu S, Yelekci K, özgen ö, Ucar G, Erol K, Kendi E, Yesilada A. *Bioorg Med Chem*, 2009, **17**: 675

32 Barsoum F F, Hosni H M, Girgis A S. *Bioorg Med Chem*, 2006, **14**: 3929

33 Ji S J, Shi H B. *Dyes Pigments*, 2006, **70**: 246

34 Wei X Q, Yang G, Cheng J B, Lu Z Y, Xie M G. *Opt Mater*, 2007, **29**: 936

35 Li J-T, Zhang X-H, Lin Z -P. *Beilstein J Org Chem*, 2007, **3**: 13

36 Levai A. *ARKIVOC*, 2005: 344

37 Kidwai M, Kukreja S, Thakur R. *Lett Org Chem*, 2006, **3**: 135

38 Fazaeli R, Aliyan H, Bordbar M, Mohammadi E. *The Open Catal J*, 2010, **3**: 79

39 Fazaeli R, Aliyan H, Mallakpour S, Rafiee Z, Bordbar M. *Chin J Catal*, 2011, **32**: 582

40 Fazaeli R, Tangestaninejad S, Aliyan H, Moghadam M. *Appl Catal A*, 2006, 309: 44

41 Fazaeli R, Tangestaninejad S, Aliyan H. *Appl Catal A*, 2007, **318**: 218

42 Fazaeli R, Aliyan H. *Appl Catal A*, 2007, **331**: 78

43 Sun M, Zhang J, Cao C, Zhang Q, Wang Y, Wan H. *Appl Catal A*, 2008, **349**: 212

44 Wiley R H, Jarboe C H, Hayes F N, Hansbury E, Nielsen J T, Callahan P X, Sellars M C. *J Org Chem*, 1958, **23**: 732

45 Mizuno N, Tateishi M, Iwamoto M. *Appl Catal A*, 1995, **128**: L165

46 Sing K S W, Everett D H, Haul R A W, Moscou L, Pierotti R A, Rouquerol J, Siemieniewska T. *Pure Appl Chem*, 1985, **57**: 603

47 Beck J S, Vartuli J C, Roth W J, Leonowicz M E, Kresge C T, Schmitt K D, Chu C T W, Olson O H, Sheppard E W. *J Am Chem Soc*, 1992, **114**: 10834

48 Kresge C T, Leonowicz M E, Roth W J, Vartuli J C, Beck J S. *Nature*, 1992, **359**: 710